A Comparison of Driving Forces for Smoke Movement in Buildings

FREDERICK W. MOWRER,* JAMES A. MILKE AND JOSE L. TORERO†

Department of Fire Protection Engineering
University of Maryland
College Park, MD 20742-3031, USA

ABSTRACT: It has been suggested that automatic shutdown of mechanical ventilation systems upon smoke detection may be superfluous and unnecessary because other driving forces will continue to transport smoke throughout buildings after the ventilation systems have been shut down. To evaluate this hypothesis, an analysis is presented that considers the relative smoke concentrations throughout a building arising from the driving forces of stack effect, wind effect, and buoyancy of combustion gases as well as those arising from mechanical ventilation. This analysis considers a representative 10-story building, but the approach presented can be extended to buildings of different heights and areas. The results of this study indicate that the shutdown of mechanical ventilation may not prevent the smoke contamination of nonfire floors, but it may still be preferable to leaving ventilation systems running unless the systems are specifically designed for smoke management.

KEY WORDS: Smoke movement, smoke management, mechanical ventilation.

INTRODUCTION

VIRTUALLY SINCE CENTRAL heating, ventilating, and air conditioning (HVAC) systems using air ducts were first introduced into commercial buildings, the potential for these systems to convey smoke, hot gases, and flames from area to area has been recognized and regulated [1,2]. Typically, this regulation has included a requirement for the installation of smoke detectors at specified locations within air distribution systems to automatically stop fans upon the detection of smoke within the air distribution system. The purpose of this requirement is to prevent a ventilation system from actively circulating smoke throughout a building. This requirement

*Author to whom correspondence should be addressed. E-mail: fmowrer@eng.umd.edu
†Currently at the University of Edinburgh, Scotland, UK

1042-3915/04/04 0237–28 $10.00/0 DOI: 10.1177/1042391504042453

does nothing, however, to prevent the movement of smoke through the air distribution system and other pathways as a result of other driving forces, including stack effect, wind effect, buoyancy of combustion gases, and fire gas expansion. Consequently, the value of automatically shutting down fans upon duct smoke detection will depend on the comparative driving forces motivating smoke flow through a building.

The purpose of this paper is to evaluate and compare the different forces motivating the movement of air and smoke during building fires. This paper describes the methodology that is used for this evaluation and presents this methodology in terms of example calculations for an example building. The approach uses recognized driving force relations in a parametric analysis to evaluate and compare effects of these driving forces for the chosen example. Based on the approach presented here, the methodology can be readily applied to a broader range of building configurations and environmental conditions.

DRIVING FORCES

The forces driving the flow of gases in buildings include [3]:

- Stack effect
- Wind effect
- Buoyancy of combustion gases
- Expansion of combustion gases
- Mechanical ventilation systems
- Elevator piston effect

Of these, stack effect, wind effect, buoyancy and mechanical ventilation are most significant under quasi-steady fire conditions, with gas expansion and elevator piston effect being important under a limited range of scenarios. In order to evaluate these effects in detail for a particular building, computer modeling is generally necessary to adequately represent the details of a building and the combinations of the different driving forces. The CONTAM model [4] is widely used for such detailed analyses.

For the present analysis, a relatively simple building geometry is used to demonstrate the relative effects of these different forces. The building is a 10-story building with 3.0 m (10 ft) floor-to-floor heights and a footprint of 30 m by 30 m (100 ft by 100 ft). The representative floor plan is shown in Figure 1. A representative section for the 10-story building is shown in Figure 2.

The specific geometry of a floor plan is not critical to the parametric analysis being performed. A rectangular floor plan is used, with four sides designated as Sides A, B, C and D, as shown in Figure 1. When wind effects are addressed, Side A will be the windward side of the building, Side B will

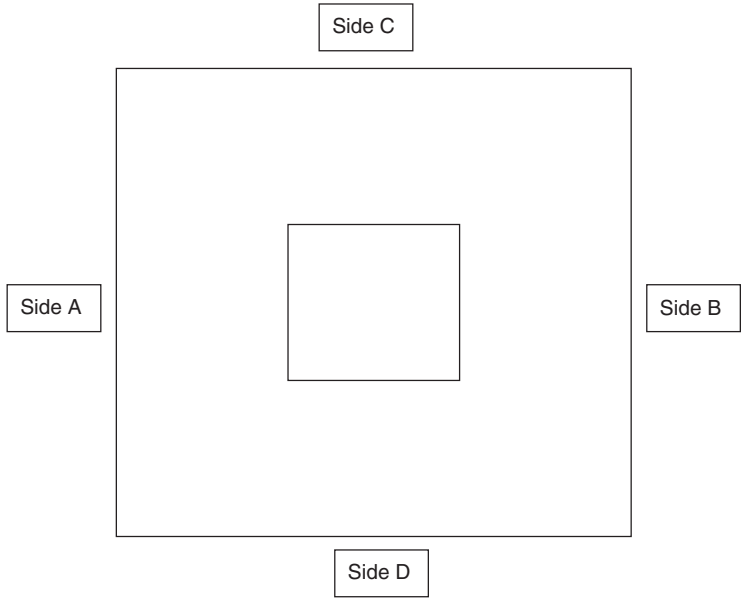

Figure 1. *Representative floor plan of building used for analysis.*

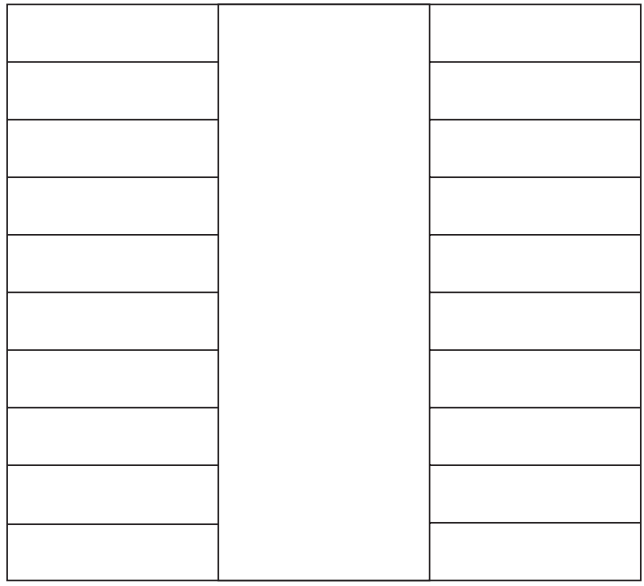

Figure 2. *Section of 10-story building used for analysis.*

be the leeward side and Sides C and D will be the lateral sides, although this can be varied through specification of appropriate wind pressure coefficients. Each side will have a specified perimeter length, L_w (m). The wall area per side is then calculated as:

$$A_w = L_w \cdot H \tag{1}$$

where H is the building height (m). The leakage areas through exterior walls are calculated as:

$$A_o = \frac{A_l}{A_w} A_w = \frac{A_l}{A_w} \cdot L_w \cdot H \tag{2}$$

where A_l/A_w is the leakage area ratio. Klote and Milke [3] tabulate typical leakage area ratios for different construction elements in commercial buildings based on the tightness of the construction. This table is duplicated as Table 1.

Klote and Milke [3] describe a methodology for evaluating the effective flow area for two paths in series, which is representative of the condition being evaluated here, i.e., leakage paths between the exterior and the interior, A_{ei}, and between the interior and the vertical shafts, A_{si}. For two paths in series, the effective flow area can be expressed as:

$$A_{eq} = \frac{A_1 A_2}{\sqrt{A_1^2 + A_2^2}} \tag{3}$$

Table 1. Typical leakage area ratios in commercial buildings [3].

Construction Element	Tightness	Leakage Area Ratio
Exterior building walls	Tight	0.70×10^{-4}
	Average	0.21×10^{-3}
	Loose	0.42×10^{-3}
	Very loose	0.13×10^{-2}
Stairwell walls	Tight	0.14×10^{-4}
	Average	0.11×10^{-3}
	Loose	0.35×10^{-3}
Elevator shaft walls	Tight	0.18×10^{-3}
	Average	0.84×10^{-3}
	Loose	0.18×10^{-2}
Floors	Tight	0.66×10^{-5}
	Average	0.52×10^{-4}
	Loose	0.17×10^{-3}

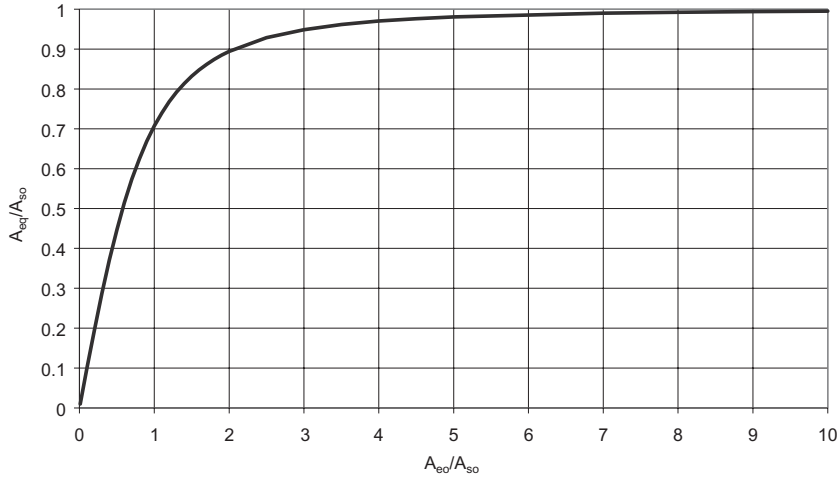

Figure 3. *Equivalent opening area ratios.*

For the two leakage paths in series being considered here, A_{si} and A_{ei}, this relationship can be expressed in nondimensional terms as:

$$\frac{A_{eq}}{A_{si}} = \frac{A_{ei}}{\sqrt{A_{si}^2 + A_{ei}^2}} = \frac{1}{\sqrt{1 + (A_{si}/A_{ei})^2}} \tag{4}$$

This relationship is illustrated in Figure 3. From Figure 3 as well as from Equation (4), the following observations can be made. For very small shaft leakage areas relative to exterior wall leakage areas, the equivalent opening area approaches the shaft leakage area. At the other extreme, for very large shaft leakage areas relative to exterior wall leakage areas, the equivalent opening area approaches the exterior wall leakage area. When these leakage areas are of comparable magnitude, then the equivalent opening area should be determined from Equation (4).

Klote and Milke [3] suggest that the ratio between shaft leakage area, A_{si}, and exterior leakage area, A_{ei}, typically ranges from about 1.7 to 7 for buildings with inoperable windows. These values suggest that most of the resistance to flow occurs between the exterior walls and the interior rather than between the interior and the shafts. Consequently, little error is introduced by setting the equivalent leakage area to the exterior leakage area for buildings with inoperable windows. For example, for $A_{si}/A_{ei} = 1.7$, the error introduced by this approximation is only 16%, while for $A_{si}/A_{ei} = 7$, the error is only 1%. Furthermore, this approximation does not account for vent openings and door gaps in shafts, which would tend to increase this

ratio further to reduce the error even more. For the present analysis, the interior resistance to flow is neglected and the equivalent leakage area is considered to be equal to the exterior leakage area. This simplifies the analysis while introducing little error.

Stack Effect

The first driving force to be evaluated is stack effect. Stack effect is a form of buoyancy-induced flow that arises as a result of differences between inside and outside temperatures. Stack effect is a linear function of building height and is most pronounced in tall buildings under winter weather conditions when the difference between inside and outside temperatures is greatest. Normal stack effect occurs when the inside temperature is greater than the outside temperature; under normal stack effect, the warmer inside air flows out of the building through high leakage paths as a result of buoyant forces, while colder outside air is drawn into the building through low pathways. Reverse stack effect occurs when the outside temperature is greater than the inside temperature; under reverse stack effect, the flow patterns described for normal stack effect are reversed. Reverse stack effect is most pronounced in very hot climates or in refrigerated buildings. This discussion will be restricted to normal stack effect.

Flows induced by stack effect result from pressure differentials that arise between spaces. The general flow patterns and pressure differences arising from normal stack effect are illustrated in Figure 4. The derivation of the quasi-steady flow balance for stack effect is presented by Klote and

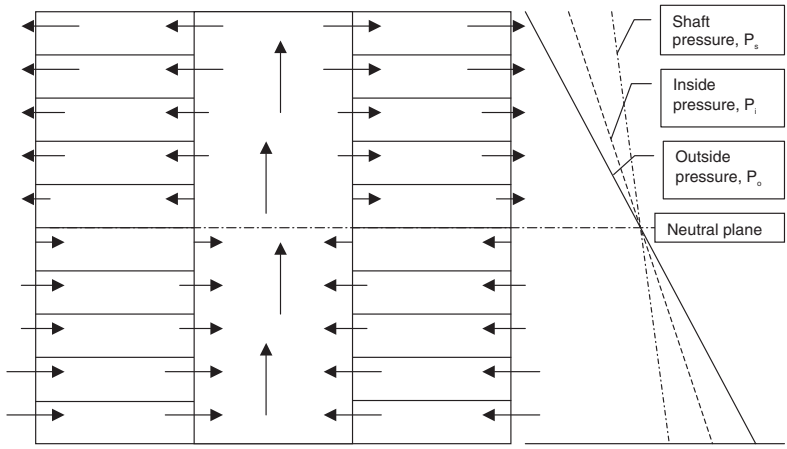

Figure 4. *Schematic diagram of pressures and flow patterns during normal stack effect.*

Milke [3]. For a shaft with continuous openings, the steady total mass inflow and outflow rates can be expressed as:

$$\dot{m}_i = \frac{2}{3} C W_o H_n^{3/2} \sqrt{2\rho_o b} \tag{5}$$

$$\dot{m}_o = \frac{2}{3} C W_o (H - H_n)^{3/2} \sqrt{2\rho_s b} \tag{6}$$

where

$$b = \frac{g P_{\text{atm}}}{R} \left[\frac{1}{T_o} - \frac{1}{T_s} \right] \tag{7}$$

and

$$\frac{H_n}{H} = \frac{1}{1 + (T_s/T_o)^{1/3}} \tag{8}$$

The relative location of the neutral plane, H_n/H, is plotted in Figure 5 as a function of the absolute temperature ratio, T_s/T_o. Figure 5 illustrates the relative insensitivity of the neutral plane location to the absolute temperature ratio for temperature ratios representative of stack effect. The relative neutral plane location only varies from 0.5 to 0.47 over a range of absolute temperature ratios from 1.0 to 1.5. An extreme case of an absolute temperature ratio for stack effect can be considered by means of an example

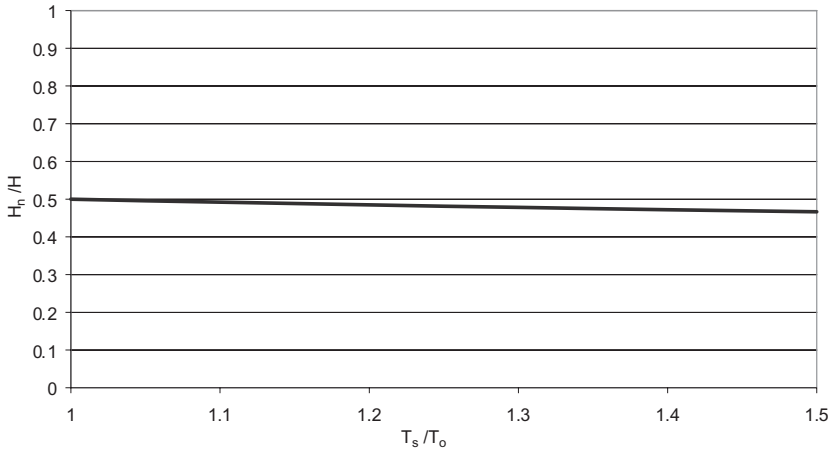

Figure 5. *Relative neutral plane location as function of absolute temperature ratio.*

where the inside temperature is a relatively balmy 30°C (303 K) and the outside temperature is a relatively frigid −30°C (243 K). For this case, the absolute temperature ratio would be 1.25. This value will be exceeded only under extremely unusual conditions for normal stack effect, but may be exceeded under fire conditions where higher interior temperatures might occur.

The total mass flow rate through a continuous vertical opening can be expressed nondimensionally as a function of the absolute temperature ratio, T_s/T_o, as:

$$\frac{\dot{m}}{\rho_o C A_o \sqrt{2gH_o}} = \frac{2}{3}\sqrt{\frac{(1 - T_o/T_s)}{(1 + (T_s/T_o)^{1/3})^3}} \tag{9}$$

The denominator on the left hand side of Equation (9) represents the mass flow rate that would occur if the entire vent area were pressurized at a value of $\sqrt{2gH_o}$. As illustrated in Figure 4, this is not the case, so the actual flow rate will only be some fraction of this theoretical flow rate, as illustrated in Figure 6. Figure 6 shows that the mass flow rate is very sensitive to the absolute temperature ratio for relatively small temperature ratios, which are representative of stack effect. Figure 6 also illustrates that the mass flow rate becomes relatively insensitive to the absolute temperature ratio for ratios above 1.5, remaining at a value within 10% of 0.13 at these higher temperature ratios, which are more representative of fire conditions in a building.

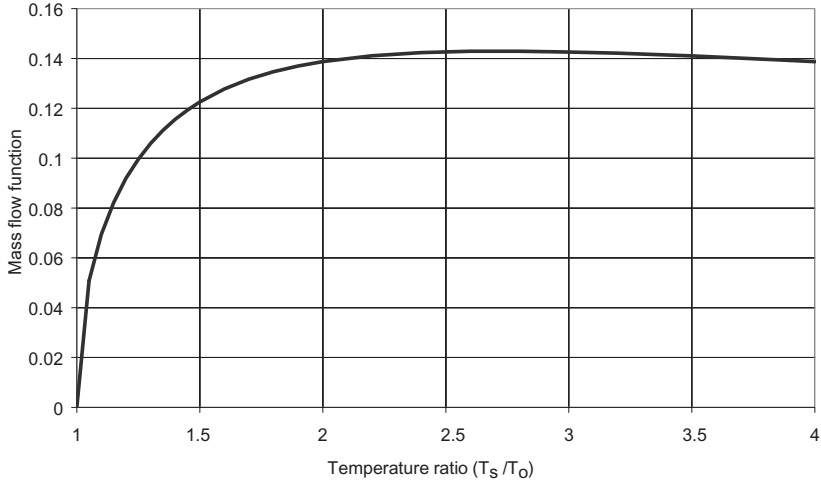

Figure 6. *Nondimensional mass flow rate as function of absolute temperature ratio.*

Stack effect is most significant as a potential mechanism for smoke spread within a building when the fire floor is located below the neutral plane. In the absence of other driving forces (e.g., when the smoke is at the inside air temperature and there is no wind), smoke on the fire floor will be drawn into vertical shafts and will flow from the vertical shafts to floors located above the neutral plane as illustrated in Figure 4. To determine the relative magnitudes of the flows caused by stack effect on each floor, Equations (5) and (6) can be applied incrementally for each floor. A spreadsheet template was developed to perform these calculations.

As an example calculation, the 10-story building described above was used, with the inside temperature set to 20°C (293 K; 68°F) and the outside temperature set to −20°C (253 K; −4°F). Average tightness was assumed for the exterior walls, so that the leakage area for each exterior wall was calculated, using the appropriate leakage value from Table 1, as:

$$A_{ei} = \frac{A_l}{A_w} A_w = (0.21 \times 10^{-3}) \cdot 30\,\text{m} \cdot 30\,\text{m} = 0.19\,\text{m}^2 \tag{10}$$

Assuming this leakage area is distributed equally over the height of the building, the leakage path width for each wall was calculated as:

$$W_o = A_{ei}/H = 0.19\,\text{m}^2/30\,\text{m} = 6.3 \times 10^{-3}\,\text{m} \tag{11}$$

Since all four walls have the same dimensions for this example, the total leakage area would be $0.76\,\text{m}^2$ and the total leakage path width would be 0.025 m. The results of these calculations are illustrated in Figure 7, which shows the pressure differential profile and the incremental flow rates on each floor of the 10-story building. The largest flows occur at the floors further away from the neutral plane, where the pressure differentials are the largest. The total flow rate for this example is 1.39 kg/s, which can also be determined from Equations (5) or (6).

In theory, a uniform concentration of smoke will develop on all upper floors under steady conditions as a result of stack effect. The steady-state relative concentration of smoke on the upper floors can be determined simply as:

$$\frac{C_{\text{uf}}}{C_{\text{ff}}} = \frac{\dot{m}_{\text{ff}}}{\dot{m}_{\text{tot}}} \tag{12}$$

where the subscript uf refers to upper floors, located above the neutral plane, and the subscript ff refers to fire floor, located below the neutral plane. Equation (12) assumes that inflow from floors other than the fire

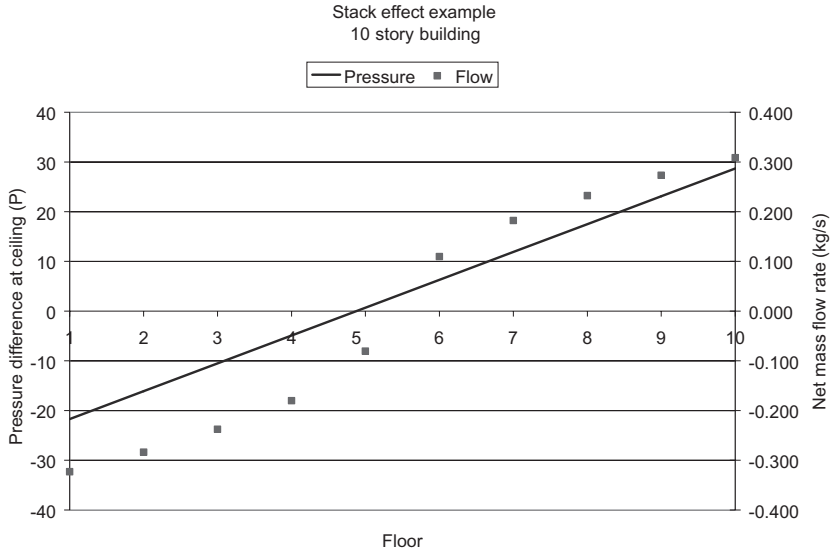

Figure 7. *Stack effect example calculation for a 10-story building.*

Table 2. Relative, upper-floor smoke concentrations.

Fire Floor	Mass Flow Rate (kg/s)	C_{uf}/C_{ff}
1	0.404	0.291
2	0.355	0.256
3	0.297	0.215
4	0.225	0.162
5	0.106	0.077
Total	1.387	–

floor located below the neutral plane will act to dilute the smoke generated on the fire floor as it moves vertically through shafts in the building before flowing from these shafts to the upper floors located above the neutral plane. It also assumes that there will be no flow from floors above the neutral plane into the shaft.

For the example calculation, the relative concentrations are provided in Table 2, where the last column shows the relative smoke concentration that would be expected on the upper floors as a result of a fire on the fire floor.

The concentrations shown in Table 2 are the values that will ultimately be achieved under steady-state conditions. The time required to achieve these steady-state concentration values will vary based on the flow rates to each

upper floor located above the neutral plane. Because the higher floors have higher flow rates as illustrated in Figure 7, they will reach steady-state concentrations more quickly. Assuming steady concentrations of smoke within the shafts feeding the upper floors, the concentration of smoke on a floor can be estimated as a function of time as:

$$\frac{C_{\mathrm{uf}}(t)}{C_{\mathrm{uf}}(ss)} = 1 - e^{-t/\tau} \tag{13}$$

where $\tau = m_{\mathrm{uf}}/\dot{m}_{\mathrm{uf}} = \rho_{\mathrm{uf}} V_{\mathrm{uf}}/\dot{m}_{\mathrm{uf}} = \rho_i A_f H_f/\dot{m}_{\mathrm{uf}}$ is a characteristic time constant and $\dot{m}_{\mathrm{uf}}$ is the mass flow rate to the individual upper floor of interest, as illustrated in Figure 7. For example, for the 10th floor, the mass flow rate is 0.386 kg/s, while the mass of air on the floor is approximately 3240 kg. Therefore, the characteristic time constant for the 10th floor would be 8394 s or 2.3 h. For the other upper floors, the mass flow rates are lower than on the 10th floor, so their time constants would be even longer than this. The relationship expressed by Equation (13) is illustrated in Figure 8. In one time constant, the concentration of gases on an upper floor will be 62.8% of the steady-state value. Thus, for this example it would take about 2 h and 20 min for the smoke concentration on the 10th floor to reach 62.8% of its steady-state value, which in turn would range from 7.7 to 29.1% of the value on the fire floor, depending on which floor is the fire floor. The rate of hazard development as well as the steady-state hazard represented by these values will depend on the magnitude of the smoke concentration on the fire floor.

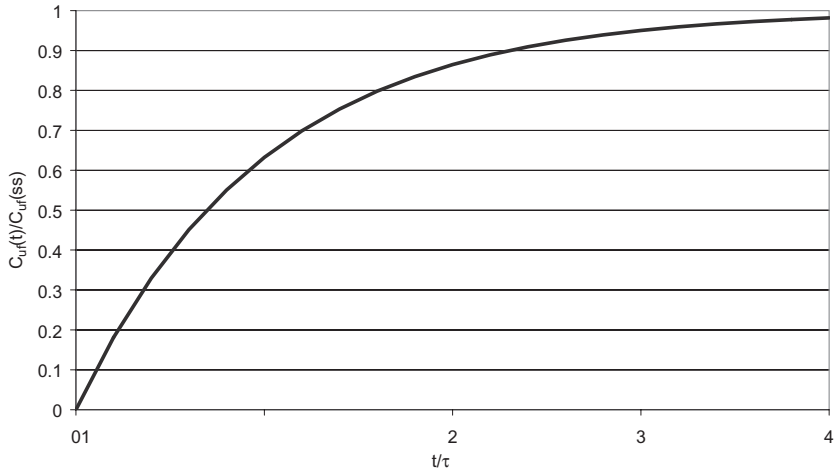

Figure 8. *Transient development of smoke concentrations on upper floors.*

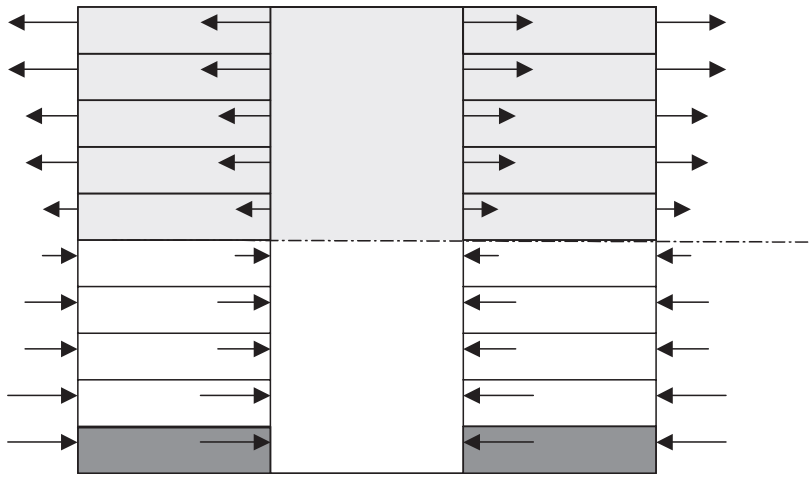

Figure 9. *Qualitative steady-state conditions resulting from fire on first floor due to stack effect.*

Figure 9 qualitatively illustrates the steady-state conditions that would develop as a result of stack effect from a fire on the first floor for the 10-story example.

Wind Effects

As noted by Klote and Milke [3], wind can have a pronounced effect on smoke movement by exerting pressures on the exterior surfaces of a building. The wind pressure exerted on a surface can be expressed as:

$$\Delta P_w = \frac{1}{2} C_w \rho_o V_w^2 \tag{14}$$

where C_w is a dimensionless pressure coefficient with a theoretical range from -1.0 to $+1.0$ and a practical range from about -0.8 to $+0.8$. Positive coefficients are associated with windward surfaces and negative coefficients are associated with leeward and lateral surfaces. For relatively tall buildings with approximately square floor plans, Klote and Milke [3; Table 5.3] suggest that the appropriate pressure coefficients will be approximately $+0.8$ on the windward face, -0.25 on the leeward face and -0.8 on the two lateral faces, as illustrated in Figure 10.

In general, wind velocities and directions will be variable with time and elevation. They can also be significantly affected by local terrain, particularly in congested urban areas with surrounding high-rise buildings.

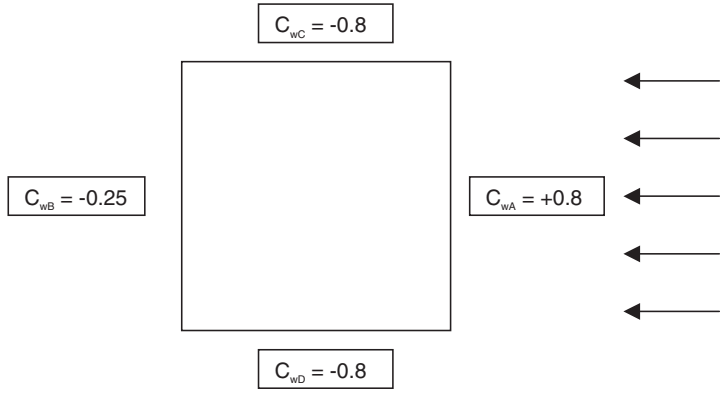

Figure 10. *Dimensionless pressure coefficients for wind pressures on building surfaces.*

For purposes of this analysis, a steady wind speed of 10 m/s (32.7 ft/s or 22 mph) is considered. This wind is assumed to apply for the full height of the building, although wind speeds tend to decrease near ground level due to boundary layer effects in reality. For this example, the wind pressure on the windward side of the building is calculated as:

$$\Delta P_w = \frac{1}{2} C_w \rho_o V_w^2 = \frac{1}{2}(0.8)(1.38\,\text{kg/m}^3)(10\,\text{m/s})^2 = 55.1\,\text{Pa} \qquad (15)$$

By similar calculation, the wind pressure would be -17.2 Pa on the leeward side and -55.1 Pa on the two lateral sides of the building. These pressures are added to the outside static pressure to provide the effective outside pressure on each face of the building, as illustrated qualitatively in Figure 11.

Figure 11 shows that the consideration of wind results in a much more complicated pressure profile and flow pattern than for the case of stack effect alone. Three separate neutral planes arise where the windward, leeward, and lateral outside pressure gradients intersect the shaft pressure gradient, with the windward pressure gradient intersecting the shaft pressure gradient relatively high in the building and the lateral and leeward pressure gradients intersecting the shaft pressure gradient relatively low in the building. In theory and in reality, the shaft and outside pressure gradients may intersect above or below the building rather than within the building height as illustrated here. This complicates matters, but is tractable and is included in the following analysis.

The same relationships that were developed for the flow through continuous openings as a result of stack effect still apply, but now they

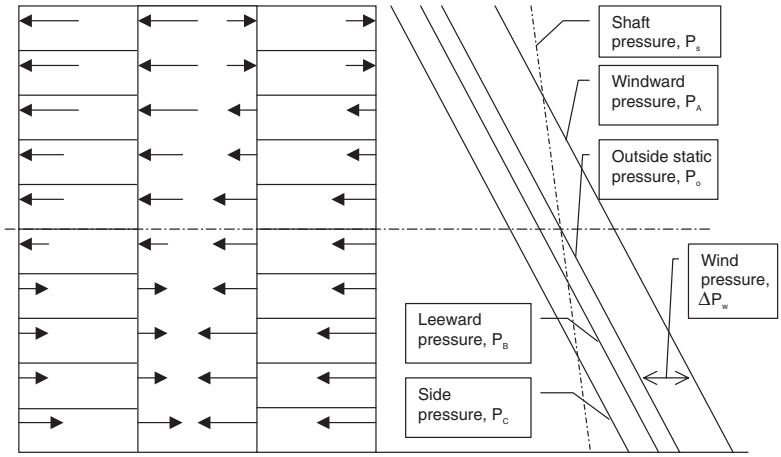

Figure 11. *Schematic diagram of pressure differentials and flow patterns resulting from combination of stack and wind effects.*

must be applied to each exterior face individually to account for the different pressure profiles on each side. The general quasi-steady mass balance can be expressed as:

$$\dot{m}_i = \dot{m}_o \tag{16}$$

The total mass inflows and outflows are equal to the sum of the mass inflows and outflows for each wall:

$$\dot{m}_i = \dot{m}_{iA} + \dot{m}_{iB} + \dot{m}_{iC} + \dot{m}_{iD} \tag{17}$$

$$\dot{m}_o = \dot{m}_{oA} + \dot{m}_{oB} + \dot{m}_{oC} + \dot{m}_{oD} \tag{18}$$

For each inflow term, Equation (5) applies, using the appropriate vent width and neutral plane height for that side of the building. For example, for Side A:

$$\dot{m}_{iA} = \frac{2}{3} C W_{oA} H_{nA}^{3/2} \sqrt{2\rho_o b} \tag{19}$$

The other three sides have similar inflow equations. Similarly, for each outflow term, Equation (6) applies, using the appropriate neutral plane height for that side of the building. For example, for Side A:

$$\dot{m}_{oA} = \frac{2}{3} C W_{oA} (H - H_{nA})^{3/2} \sqrt{2\rho_s b} \tag{20}$$

The other three sides have similar outflow equations. In order to solve the mass balance expressed by Equation (16), it is necessary to determine the elevations of the neutral pressure planes for each side of the building that provide the mass balance. Based on the linear pressure profiles assumed for each face and for the interior shaft, the neutral plane heights for each face are linearly related to each other as:

$$H_{nB} = H_{nA} + \frac{\Delta P_{wB} - \Delta P_{wA}}{(\rho_o - \rho_i)g} \tag{21}$$

$$H_{nC} = H_{nA} + \frac{\Delta P_{wC} - \Delta P_{wA}}{(\rho_o - \rho_i)g} \tag{22}$$

$$H_{nD} = H_{nA} + \frac{\Delta P_{wD} - \Delta P_{wA}}{(\rho_o - \rho_i)g} \tag{23}$$

By substituting these equations into the appropriate inflow and outflow equations, the only unknown solution variable becomes H_{nA}. An iterative approach is used to determine the elevation of H_{nA} that provides the solution for the mass balance expressed by Equation (16). This iterative approach was implemented in a spreadsheet template, which was used for the example calculations for wind effect. Once H_{nA} is known, Equation (21)–(23) are used to determine the neutral plane heights for the other sides of the building.

For situations where the elevation of a neutral plane is located above the height of the building, the mass inflow terms have to be adjusted by subtracting the flow that would be calculated to occur between the top of the building and the neutral plane. For this case, the inflow equation becomes:

$$\dot{m}_i = \frac{2}{3} C W_o \sqrt{2\rho_o b}\left[H_n^{3/2} - (H_n - H)^{3/2}\right] \tag{24}$$

Similarly, for situations where the elevation of a neutral plane is located below the base of the building, the mass outflow terms have to be adjusted by subtracting the flow that would be calculated to occur between the neutral plane and the bottom of the building. For this case, the outflow equation becomes:

$$\dot{m}_o = \frac{2}{3} C W_o \sqrt{2\rho_s b}\left[(H - H_n)^{3/2} - (-H_n)^{3/2}\right] \tag{25}$$

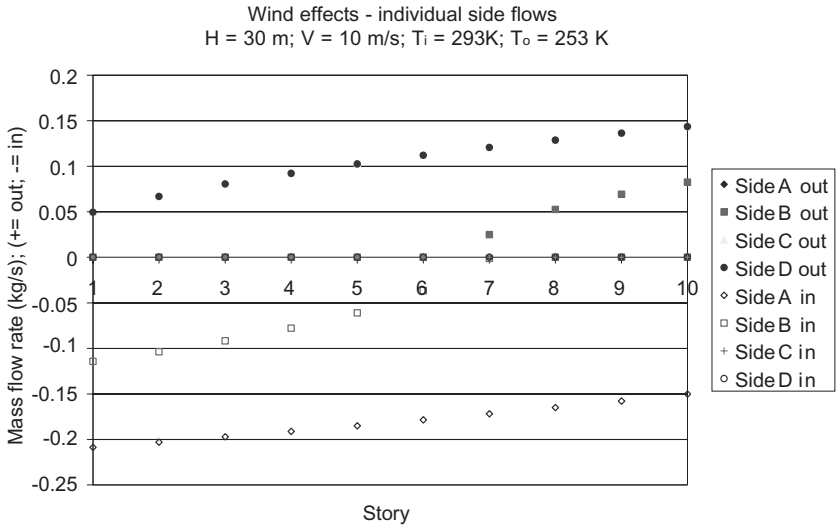

Figure 12. *Results of example calculation of wind effects for 10-story building.*

The example calculation for wind effect is the same calculation used for the stack effect example presented, but with a 10 m/s wind impinging perpendicular to Side A of the building. The results of this calculation are illustrated in Figure 12.

The results for Side C do not appear in Figure 12 because they are masked by the results for Side D, which are identical for this example. Some observations regarding this example calculation can be made. First, the neutral plane elevation on Side A is at 57.6 m, which is 1.92 times the height of the building, while the neutral plane elevation for Sides C and D are at −2.2 m, just below the base of the building. As a consequence of these neutral plane locations, Side A has inflow for its entire height, while Sides C and D have outflow for their entire heights. Side B, the leeward side of the building, has a neutral plane elevation of 18.3 m for this calculation, an elevation near the floor level of the 7th floor. Below this elevation, Side B has inflow, while above this elevation, Side B has outflow, as illustrated in Figure 12.

Figure 13 is a sectional view of the 10-story building showing the different flow rates for each floor for the wind effects example. These are not the flow rates for each side of the building, but rather the total inflow and outflow rates for each floor, along with the net flow rates between floors in the shafts. The values in the left hand column are the mass outflow rates for each story, while the values in the right hand column are the mass inflow rates for each story. The values in the center column represent the net flow

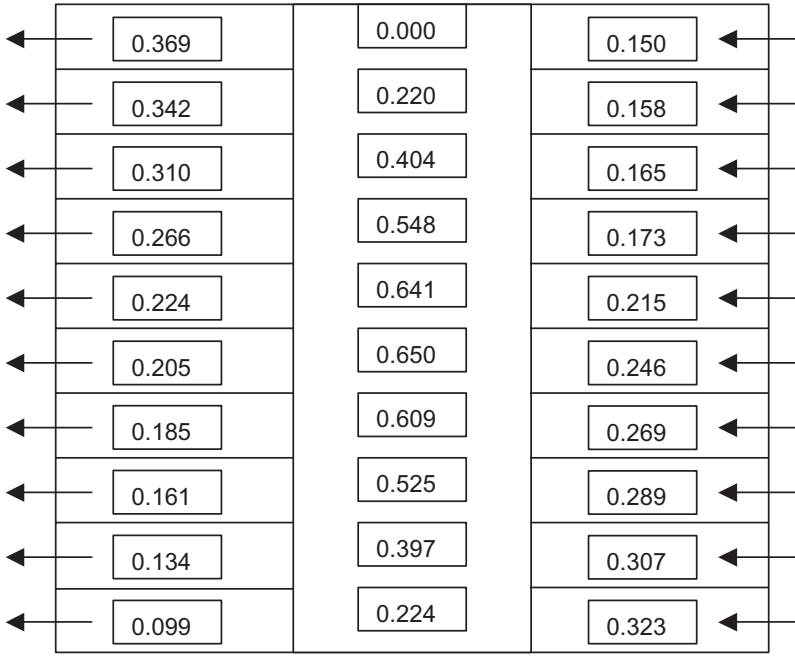

Figure 13. *Schematic of mass flows in 10-story example building with wind effects.*

rate in the shafts entering from the floor below. All values are expressed in units of kg/s.

Estimating smoke concentrations throughout a building as a result of the combined effects of stack effect and wind effect is more complicated than for the case of stack effect alone, although the general relationship expressed by Equation (12) still applies. Unlike for stack effect, where the flow on any floor is either into a shaft from the interior space or out of a shaft into the interior space, for wind effect combined with stack effect many floors have a flow through arrangement as illustrated in Figure 13. Under these circumstances, evaluation of smoke concentrations must be treated differently.

Two approaches are presented for estimating smoke concentrations under the combined influences of stack and wind effects. The first approach assumes perfect mixing at each floor, while the second approach assumes no smoke flow on floors where the inflow of air through walls is greater than the outflow of air on that floor. For the second approach, the excess flow on floors where the inflow exceeds the outflow is assumed to enter the shaft and dilute the smoke within the shaft.

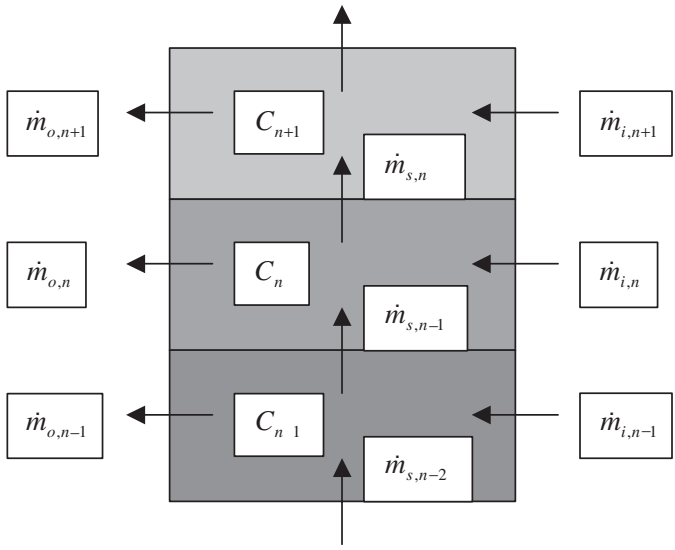

Figure 14. *Smoke concentration terms for the perfect mixing model.*

For the first case of perfect mixing, it is assumed that smoke rises through a shaft and perfectly mixes with the air entering each floor. The outflowing stream is assumed to be smoke with a concentration the same as on the associated floor. This concept is illustrated in Figure 14. The concentration of smoke on the fire floor is assumed to be unity, i.e., $C_{\mathrm{ff}} = 1$, such that all other concentrations are relative to the smoke concentration on the fire floor. In general, the concentration of smoke on a floor is calculated for the perfect mixing model as:

$$\frac{C_n}{C_{n-1}} = \frac{\dot{m}_{s,\,n-1}}{\dot{m}_{s,\,n-1} + \dot{m}_{i,\,n}} \tag{26}$$

Consider, for example, a fire on the first floor of a 10-story building. This floor is being provided with 0.323 kg/s of air from the outside to support the combustion process and generate smoke. Of this, 0.099 kg/s leaves the building on the first floor, while 0.224 kg/s flows to the second floor. At the second floor, the 0.224 kg/s of smoke from the first floor is diluted with 0.307 kg/s of air flowing into the building through the second floor. This dilutes the smoke from the first floor in accordance with Equation (12) as:

$$\frac{C_2}{C_1} = \frac{\dot{m}_{\mathrm{ff}}}{\dot{m}_{\mathrm{tot}}} = \frac{0.224}{0.224 + 0.307} = 0.42 \tag{27}$$

Similarly, the smoke flowing from the second floor to the third floor will enter the third floor with a concentration C_2, then will be diluted by the air flowing into the building through the third floor. This is expressed mathematically as:

$$\frac{C_3}{C_1} = \frac{C_2}{C_1}\frac{C_3}{C_2} = \frac{C_2}{C_1}\frac{\dot{m}_2}{\dot{m}_{\text{tot}}} = 0.42\frac{0.397}{0.397 + 0.289} = 0.42 \times 0.58 = 0.243 \quad (28)$$

This process continues for each additional story.

For the second approach, called the no mixing approach, smoke enters a floor from the shaft only if the outflow from the floor is greater than the inflow through exterior openings. Under these circumstances, smoke would flow from the shaft to the floor to make up the difference between the wall outflow and inflow. If the inflow on a floor is greater than the outflow from the floor, then it is assumed that no smoke flows from the shaft to that floor and the excess inflow to the floor would flow into the shaft and dilute the smoke in the shaft. These concepts are illustrated in Figure 15.

For the middle floor shown in Figure 15, the mass inflow is greater than the mass outflow. Consequently, the smoke concentration on the floor is assumed to be zero, while the concentration of smoke within the shaft is diluted by the flow from the floor into the shaft. In general, this dilution can be expressed as:

$$\frac{C_{s,n}}{C_{s,n-1}} = \frac{\dot{m}_{s,n-1}}{\dot{m}_{s,n-1} + \dot{m}_{i,n} - \dot{m}_{o,n}} \quad (29)$$

For the upper floor shown in Figure 15, the mass outflow is greater than the mass inflow, with the difference made up with the flow of smoke from

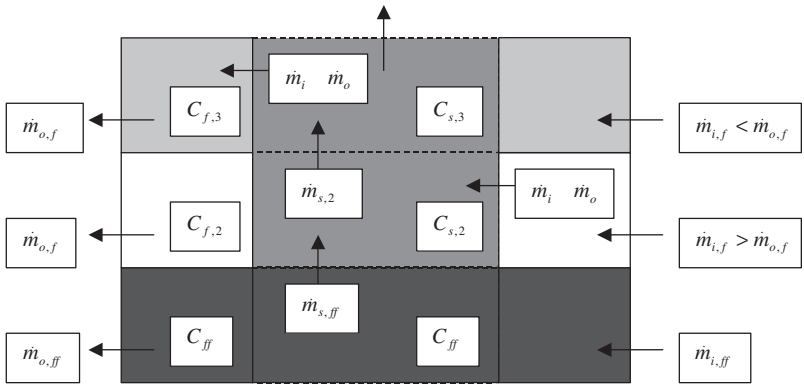

Figure 15. *Smoke concentration concepts for the no mixing model.*

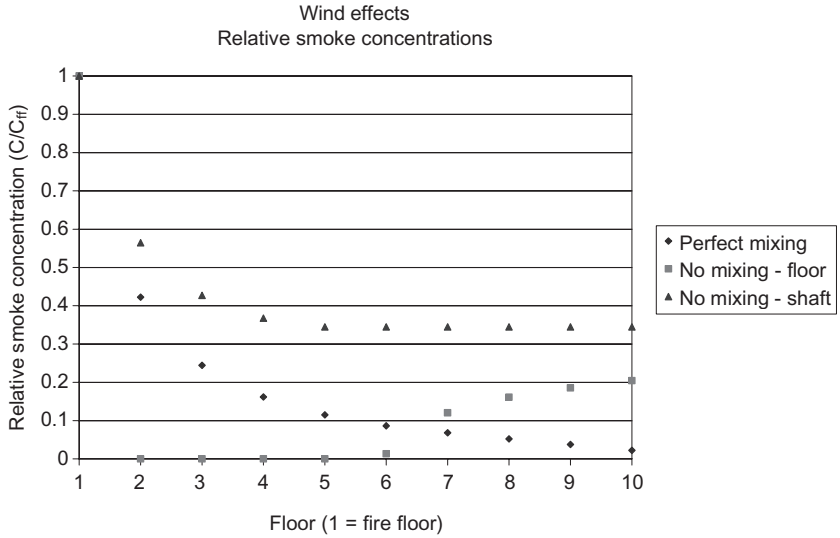

Figure 16. *Relative smoke concentrations per floor from stack and wind effects.*

the shaft to the floor. The concentration of smoke flowing from the shaft onto the floor will be diluted by the air flowing into the floor through the wall, while the concentration of smoke in the shaft is the same as in the shaft on the floor below because no air is entering the shaft to dilute the smoke. In general, the dilution on the floor relative to the shaft can be expressed as:

$$\frac{C_{f,n}}{C_{s,n}} = \frac{\dot{m}_{o,n} - \dot{m}_{i,n}}{\dot{m}_{o,n} - \dot{m}_{i,n} + \dot{m}_{i,n}} = \frac{\dot{m}_{o,n} - \dot{m}_{i,n}}{\dot{m}_{o,n}} = 1 - \frac{\dot{m}_{i,n}}{\dot{m}_{o,n}} \tag{30}$$

For the flow patterns shown in Figure 13, the relative smoke concentrations on each floor are shown in Figure 16 for the perfect mixing and the no mixing models for smoke spread under the influence of stack and wind effects. The smoke concentrations in the shaft are also shown for the no mixing model. The perfect mixing model demonstrates a diminishing concentration of smoke at each floor level, with dilution occurring at each floor level. The no mixing model is more similar to the stack effect case, with no smoke entering floors 2 through 5 and increasing concentrations of smoke entering floors 6 through 10. This is somewhat different from the stack only case, where smoke concentrations above the neutral plane were uniform.

Buoyancy Effects

Buoyancy forces associated with hot fire gases in an enclosure are fundamentally the same as those associated with stack effect. The primary

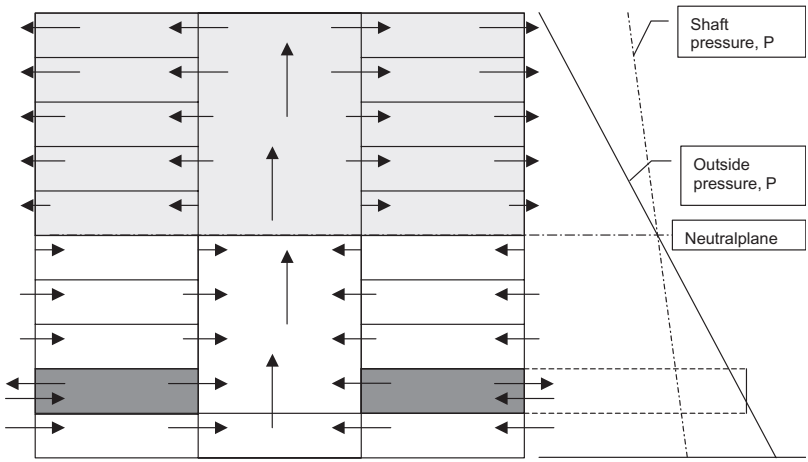

Figure 17. *Schematic diagram of pressures and flow patterns due to buoyancy and stack effects.*

difference is that fire gas buoyancy typically involves much larger density differences and much smaller vertical differences. For this discussion, consider the sectional view and pressure profiles shown in Figure 17.

A basic assumption used for this analysis is that the interior pressure on each floor is essentially the same as the shaft pressure because the shaft leakage area is assumed to be much larger than the exterior wall leakage area. If and when windows break on the fire floor, this assumption no longer holds on the fire floor. Instead, the background pressure on the fire floor will approach the outside pressure, particularly if the area of broken windows becomes much larger than the shaft leakage area on the fire floor. On the fire floor, a second neutral plane will develop at the elevation where the flow rate to the fire floor becomes equal to the smoke flow from the fire floor. This will typically be near the mid-height of the fire floor. Below this fire floor neutral plane, air will flow to the fire floor from the outside, while above this elevation, smoke will flow from the fire floor to the outside.

The flow of smoke from the fire floor to the shaft will be driven by essentially the same pressure differential as for the case of stack effect only. The flow rate of smoke into the shaft will depend on the area of the openings between the shaft and the fire floor. Relative to the stack only case, the flow rate of smoke into the shaft on the fire floor when windows on the fire floor are broken can be estimated as:

$$\frac{\dot{m}_{\text{buoy}}}{\dot{m}_{\text{stack}}} \approx \frac{A_{si}}{A_{ei}} \tag{31}$$

As noted previously, Klote and Milke [3] suggest that this area ratio typically varies from about 1.7 to 7. This would suggest that the flow of smoke into a shaft from a fire floor with broken windows would also vary over this same range. It is important to recognize that this discussion is based on the assumption that windows will break and fall out on the fire floor. If the exterior leakage area remains the same as for stack effect only, then the mass flow rate into the shaft will remain approximately the same as for the stack effect only case.

The combined effects of buoyancy, stack, and wind will be qualitatively similar to those for buoyancy and stack effects with respect to flow from the fire floor into the shaft and quantitatively similar to those described in the previous subsection for wind and stack effects for floors above the fire floor. Under the influence of strong winds, fires located on the windward side of a building will tend to be blown into the building, while fires located on the lateral and leeward sides of the building will tend to be drawn out of the building because the windward side will be at positive pressure relative to the interior space, while the lateral and leeward sides will be at negative pressure relative to the interior space.

Mechanical Ventilation

A simplified but representative mechanical ventilation system is shown in Figure 18. A fan with a capacity of $\dot{V}_{\text{fan}}$ distributes air approximately equally to all the floors served by the ventilation system. In modern commercial buildings mechanical ventilation systems are typically designed to produce approximately 4–6 air changes per hour. Some fraction of the air being circulated is exhausted from the building and an equal volume of makeup air is introduced into the system. The fraction of air recirculated is typically about 80–90%, with the other 10–20% being exhausted and replaced with fresh air. For this analysis, the recirculation fraction is represented as χ_{rec}.

When a fire occurs on a floor, smoke from the fire is drawn into the return duct, where it mixes with the return air from other floors. Assuming the flow rates to all floors served by the mechanical ventilation system are the same, the concentration of smoke in the return duct before dilution by the make up air will be:

$$\frac{C_{\text{ret}}}{C_{\text{ff}}} = \frac{\dot{m}_{\text{ff}}}{\dot{m}_{\text{ret}}} = \frac{1}{n} \tag{32}$$

where n represents the number of floors served by the ventilation system. This equation applies only before smoke begins to be recirculated via the

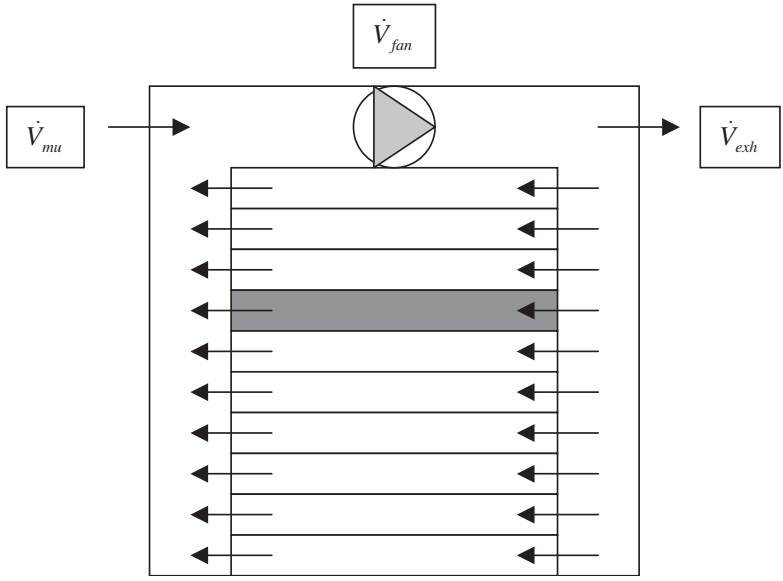

Figure 18. *Schematic diagram of representative mechanical ventilation system.*

ventilation system. Once the make up air is introduced into the return air stream, the concentration of smoke at the fan will be further diluted as:

$$\frac{C_{\text{fan}}}{C_{\text{ret}}} = \frac{\dot{m}_{\text{ret}}}{\dot{m}_{\text{ret}} + \dot{m}_{\text{mu}}} = \frac{\dot{m}_{\text{ret}}}{\dot{m}_{\text{fan}}} = \chi_{\text{rec}} \tag{33}$$

The concentration of smoke at the fan, C_{fan}, will be delivered to each floor via the supply ducts.

In theory, the concentration of smoke on the fire floor will change as smoke is recirculated back onto the fire floor as well as to other floors. For the present analysis, it is assumed that the smoke concentration on the fire floor, C_{ff}, remains constant. The concentration of smoke in the ventilation system and on other floors will be determined relative to the concentration on the fire floor.

Once smoke begins to be recirculated via the mechanical system, the concentration of smoke in the return duct can be calculated as:

$$\frac{C_{\text{ret}}}{C_{\text{ff}}} = \frac{1}{n}\left[\frac{(n-1)C_{\text{f}}}{C_{\text{ff}}} + 1\right] \tag{34}$$

where C_{f} is the smoke concentration on the nonfire floors, which is assumed to be the same on all nonfire floors due to mixing in the ventilation system.

The smoke concentration on any floor can be calculated for steady flow conditions as:

$$\frac{dC_f}{(C_{fan} - C_f)} = \frac{dt}{\tau} \tag{35}$$

where τ is the ventilation system time constant, represented as:

$$\tau = \frac{V}{\dot{V}} \tag{36}$$

As noted previously, in commercial buildings air exchange rates are typically in the range of 4–6 air changes per hour. Consequently, the time constants for such systems will range from 10 (V/6 V/h) to 15 (V/4 V/h) min.

Assuming the initial concentration of smoke on the nonfire floors is zero and the concentration of smoke on the fire floor is constant at C_{ff}, Equation (35) can be integrated as:

$$\frac{C_f}{C_{ff}} = \left(\frac{(\chi_{rec}/n)}{(1 - \chi_{rec}(n-1)/n)}\right)\left[1 - \exp\left(-(1 - \chi_{rec}(n-1)/n)\frac{t}{\tau}\right)\right] \tag{37}$$

The smoke concentration on the non-fire floors will asymptotically approach a steady-state relative smoke concentration of:

$$\frac{C_f}{C_{ff}} = \left(\frac{(\chi_{rec}/n)}{(1 - \chi_{rec}(n-1)/n)}\right) \tag{38}$$

For the 10-story building example, with a recirculation fraction of 0.9, the relative smoke concentration on the nonfire floors will achieve a steady-state value of 0.47, i.e., the smoke on the nonfire floors will ultimately reach a concentration 47% of that on the fire floor. For this example, the development of the relative smoke concentration is shown as a function of the nondimensional time, t/τ, in Figure 19.

For a mechanical ventilation rate of 4 air changes per hour, each time constant represents 15 min, so a value of t/τ equal to 4 represents a time of 1 h. Thus, for this example the relative smoke concentration on the nonfire floors would be 25.2% after 1 h, 37.0% after 2 h, 42.5% after 3 h and 45.1% after 4 h.

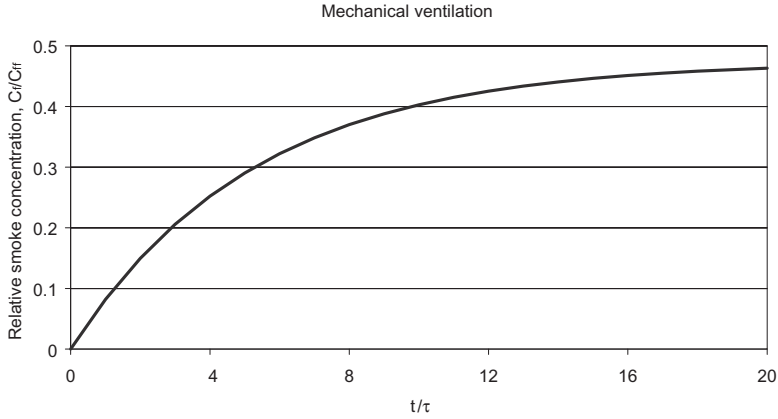

Figure 19. *Relative smoke concentration as a function of normalized time for mechanical ventilation.*

SUMMARY

A methodology has been presented for evaluating and comparing the forces driving the movement of smoke in building fires. This methodology has been demonstrated with example calculations for a 10-story building under a limited range of conditions. The methodology presented here should be generally applicable to buildings of other heights and for other conditions, but the results may be different from those presented here. The following observations and conclusions are made based on the analysis presented here for the example building. Consequently, the observations and conclusions presented below apply only to the example building and to buildings of similar configuration under similar conditions.

For the example calculations, the steady-state relative smoke concentrations associated with mechanical ventilation are higher than those associated with stack effect, with the combination of stack effect and wind effect, and with the combination of stack effect, wind effect, and buoyancy. These steady-state relative smoke concentrations are achieved more rapidly with mechanical ventilation due to the higher ventilation rates associated with mechanical ventilation compared with stack effect, wind effect, or buoyancy. Finally, these higher relative smoke conditions are achieved on all nonfire floors served by a mechanical ventilation system. For the cases of stack effect, wind effect, and buoyancy, smoke conditions are only experienced on floors located above the fire floor, with the specific floors being affected dependent on the location of the fire relative to the neutral pressure plane and the location of the nonfire floors relative to the neutral pressure plane.

Traditionally, regulations have required mechanical ventilation systems to be shut down upon smoke detection to prevent the active circulation of smoke through these systems. The analysis presented here tends to support these requirements because if mechanical ventilation systems continue to operate under fire conditions, they can circulate smoke to floors where it might not otherwise be transported, in higher concentrations and in shorter times than would occur if the ventilation system were shut down upon smoke detection. While ventilation system ducts can continue to serve as pathways for smoke transport under the influence of stack, wind, and buoyancy effects even after mechanical ventilation systems are shut down, the rate and extent of smoke transport will generally be less than if the ventilation systems continue to operate. While shutting down ventilation systems upon smoke detection might not be sufficient to prevent unacceptable levels of smoke hazard from developing on some nonfire floors, this option appears to be better than the alternative of leaving the systems running under fire conditions.

The analysis presented here does not support the suggestion that automatic shutdown of mechanical ventilation fans upon smoke detection is superfluous and therefore unnecessary in general. There may be individual circumstances where such automatic controls might be demonstrated to be unnecessary to achieve particular performance objectives. The analytical methods described here might be used to perform the analyses to support such a concept under certain circumstances. But for many situations, such as the example calculations presented here, the current requirements contained in NFPA 90A [2] and other ventilation system standards for the automatic shutdown of mechanical ventilation fans upon smoke detection have technical validity. The authors do not believe these requirements should be changed without further substantiating research to demonstrate a better alternative.

NOMENCLATURE

A_{ei} = leakage area between exterior and interior of building (m^2)
A_{eq} = equivalent leakage area for multiple leakage paths (m^2)
A_f = floor area (m^2)
A_l = leakage area (m^2)
A_o = opening area (m^2)
A_{si} = leakage area between interior space and shaft (m^2)
A_w = wall area (m^2)
b = stack effect factor defined in Equation (7)
C = orifice discharge coefficient (–)
C_f = concentration of smoke on a floor (kg/kg or kg/m^3)

C_{fan} = concentration of smoke at mechanical ventilation fan (kg/kg or kg/m^3)
C_{ff} = concentration of smoke on fire floor (kg/kg or kg/m^3)
C_{ret} = concentration of smoke in return portion of ventilation system (kg/kg or kg/m^3)
C_{uf} = concentration of smoke on upper floors (kg/kg or kg/m^3)
C_w = wind pressure coefficient (−)
g = gravitational constant (9.81 m/s^2)
H = height of building (m)
H_f = height of floor (m)
H_n = height of neutral pressure plane (m)
H_o = height of wall opening (m)
L_w = length of wall (m)
$\dot{m}$ = mass flow rate (kg/s)
$\dot{m}_{ff}$ = mass flow rate of air to fire floor (kg/s)
$\dot{m}_i$ = mass flow rate into building or space (kg/s)
$\dot{m}_o$ = mass flow rate out of building or space (kg/s)
$\dot{m}_{ret}$ = total mass flow rate of air in return portion of ventilation system (kg/s)
$\dot{m}_{tot}$ = total mass flow rate of air (kg/s)
$\dot{m}_{uf}$ = total mass flow rate to an upper floor (kg/s)
n = number of floors served by mechanical ventilation system (−)
P_{atm} = atmospheric air pressure (101,325 Pa)
P_w = wind pressure (Pa)
R = ideal gas constant (287.0 J/kg K)
T_o = absolute temperature of outside air (K)
T_s = absolute temperature of air in shaft (K)
$\dot{V}_{fan}$ = volumetric flow capacity of mechanical ventilation system (m^3/s)
V_{uf} = volume of upper floor (m^3)
V_w = wind velocity (m/s)
W_o = effective width of wall opening (m)
χ_{rec} = fraction of air recirculated in a mechanical ventilation system (–)
ρ_i = ambient density of air in building (kg/m^3)
ρ_o = ambient density of outside air (kg/m^3)
ρ_s = ambient density of air in shaft (kg/m^3)
τ = characteristic time constant (s)

REFERENCES

1. Schmidt, W.A., "Air Conditioning and Ventilating Systems," Fire Protection Handbook, 18th Edn., Section 7 / Chapter 14, National Fire Protection Association, Quincy, MA, 1997.

2. NFPA 90A, Standard for the Installation of Air Conditioning and Ventilating Systems, National Fire Protection Association, Quincy, MA, USA, 2002.
3. Klote, J.H. and Milke, J.A., Principles of Smoke Management, American Society of Heating, Refrigerating and Air-Conditioning Engineers, Inc., Atlanta, GA, USA, and Society of Fire Protection Engineers, Bethesda, MD, USA, 2002.
4. Dols, W.S., Walton, G.N. and Denton, K.R., CONTAMW 1.0 User Manual: Multizone Airflow and Contaminant Transport Analysis Software, NISTIR 6476, National Institute of Standards and Technology, Gaithersburg, MD, USA, June 2000.